

General-Chirp-Sequence Based Orthogonal Circulant Multiplexing for Short-Reach IM/DD Systems

Zhaoquan Fan ⁽¹⁾, and Jian Zhao ⁽¹⁾

⁽¹⁾ School of Electronic and Information Engineering, South China University of Technology, Guangzhou, China, zhaojian@scut.edu.cn

Abstract We propose a novel general-chirp-sequence based orthogonal circulant multiplexing (OCM) that can whiten both noise and ISI across the subcarriers, and demonstrate in 117.8-Gbit/s IM/DD experiments with 10-GHz-class devices that the proposed scheme outperforms conventional OFDM, DFT-spread OFDM, OCDM and CLPS-based OCM. ©2022 The Author(s)

Introduction

Multicarrier technology has been widely studied in short-reach intensity-modulation and direct-detection (IM/DD) data centre interconnects due to its high resistance to inter-symbol interference (ISI) [1-2]. In theory, entropy loading can maximize the channel capacity via “water filling” criterion [2]. However, this method needs precise channel state information (CSI) from the receiver, which results in a large round-trip delay and high complexity. Precoded orthogonal frequency division multiplexing (OFDM) such as discrete Fourier transform spread (DFT-S) OFDM and discrete Hartley transform precoded (DHT-P) OFDM [3] can improve the performance of frequency-selective channels without the CSI, by spreading the noise evenly over the subcarriers. However, when there is residual ISI or inter-carrier interference (ICI) due to for example nonlinear interplay between bandwidth limitation and square-law detection, prominent dips occur in the signal-to-noise-and-interference ratio (SNIR) profile, which degrades the performance.

In [4], we proposed orthogonal chirp division multiplexing (OCDM), which can not only spread the noise over subcarriers, but also enhance the tolerance to the ISI/ICI in the time-selective channel. Further investigations have been explored to identify the reason and it is found that OCDM can alleviate the dips in the SNIR profile compared to conventional precoded OFDM. However, the SNIR profile of OCDM is still not flat. In [5], we propose a novel chirp-like polyphase sequence (CLPS) based orthogonal circulant multiplexing (OCM) that can control the ISI/ICI distribution by adjusting the CLPS's parameters and thus further improve the performance by approaching the equal gain criterion [6].

In this paper, we will propose a novel general-chirp-sequence (GCS) based OCM, which can whiten the ISI in a better way and enable a flatter SNIR profile than other schemes. We demonstrate in 117.8-Gbit/s IM/DD experiments with 10-GHz-class devices that the proposed

scheme has superior performance than conventional OFDM, DFT-S OFDM, OCDM and CLPS-based OCM by using a suitable GCS.

Principle

Fig. 1 shows the principle of OCM. Instead of using DFT/IDFT in OFDM, a $N \times N$ orthogonal circulant matrix \mathbf{C} is used to multiplex/demultiplex subcarriers. The matrix \mathbf{C} is generated by circularly right shifting a basic sequence $\mathbf{c} = (c_0, c_1, \dots, c_{N-1})$ and has a form of $\mathbf{C} = [c_0, c_1, \dots, c_{N-2}, c_{N-1}; c_{N-1}, c_0, c_1, \dots, c_{N-2}; \dots; c_1, c_2, \dots, c_{N-1}, c_0]$. Therefore, OCM is fully determined by the design of the sequence \mathbf{c} . In OCDM, \mathbf{c} is a Zadoff-Chu (ZC) sequence while in CLPS-based OCM, \mathbf{c} is a CLPS. The proposed GCS in this paper is:

$$c_k = \frac{1}{\sqrt{N}} \exp\left(-j \frac{\pi\alpha}{N} k^2\right), \quad k = 1 \dots N \quad (1)$$

where α and N are relatively prime [7]. When α is 1, Eq. (1) degenerates to the ZC sequence.

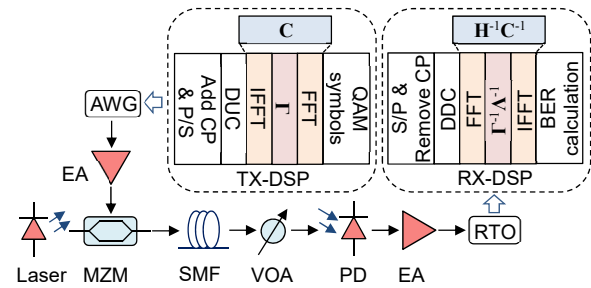


Fig. 1. Principle and experimental setup of the IM/DD OCM.

From the property that the eigenvectors of a circulant matrix comprise a discrete Fourier transform (DFT) matrix, \mathbf{C} can be decomposed as $\mathbf{C} = \mathbf{F}^{-1} \mathbf{\Gamma} \mathbf{F}$, where \mathbf{F} and \mathbf{F}^{-1} are the DFT and IDFT matrix respectively. $\mathbf{\Gamma} = \text{diag}(\mathbf{F}\mathbf{c}^T)$ is a diagonal matrix with the diagonal elements equal to the eigenvalues of \mathbf{C} , where $(\cdot)^T$ represents the transpose operation. Therefore, the multiplexing of OCM can be implemented using a pair of FFT, as shown in Fig. 1. Assuming that the i^{th} symbol before multiplexing is S_i , the multiplexed signal \mathbf{X}_i can be written as:

$$\mathbf{X}_i = \mathbf{C}\mathbf{S}_i = \mathbf{F}^{-1}\mathbf{\Gamma}\mathbf{F}\mathbf{S}_i \quad (2)$$

In IM/DD, the transmitted signal should be real and so digital up-conversion (DUC) is employed [8]. Cycle prefix (CP) is added to the OCM symbols to combat the impairments.

After detection, in the receiver DSP, the signal is synchronized and digitally down-converted (DDC). By exploiting $\mathbf{C}^{-1} = \mathbf{F}^{-1}\mathbf{\Gamma}^{-1}\mathbf{F}$, channel equalization and demultiplexing can be realized simultaneously using one-tap equalizers:

$$\mathbf{Y}_i = \mathbf{C}^{-1}\mathbf{H}^{-1}(\mathbf{R}_i + \mathbf{Z}_i + \mathbf{N}_i) = \mathbf{F}^{-1}\mathbf{\Gamma}^{-1}\mathbf{\Lambda}^{-1}\mathbf{F}(\mathbf{R}_i + \mathbf{Z}_i + \mathbf{N}_i) \quad (3)$$

where \mathbf{H} , \mathbf{R}_i , \mathbf{Z}_i , and \mathbf{N}_i represent the channel matrix, the received signal vector, the ISI/ICI vector and the noise vector, respectively. The diagonal matrix $\mathbf{\Lambda}$ represent the eigenvalues of \mathbf{H} and also the frequency response of the channel.

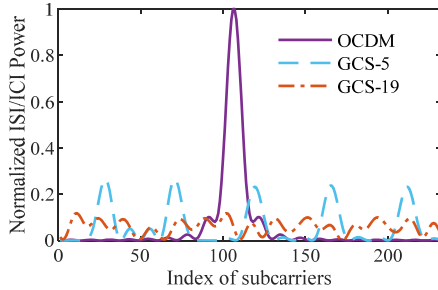


Fig. 2. Normalized ISI/ICI power versus the index of subcarriers for different α in the GCS-based OCM.

The distributions of the noise $\mathbf{C}^{-1}\mathbf{H}^{-1}\mathbf{N}_i$ and the residual ISI/ICI $\mathbf{C}^{-1}\mathbf{H}^{-1}\mathbf{Z}_i$ over subcarriers strongly influence the system performance. It can be proved that the noise can be whitened in OCM when the sequence \mathbf{c} is a constant amplitude zero autocorrelation sequence. OCDM, CLPS- and GCS-based OCM all satisfy this condition. However, the influence of ISI/ICI varies for different schemes. In order to illustrate this, we plot the distribution of the ISI/ICI power, $\mathbf{C}^{-1}\mathbf{H}^{-1}\mathbf{Z}_i$, as a function of the subcarrier index in Fig. 2. In the figure, we set \mathbf{Z}_i as $[1, 1, 1, 1, 1, 0, 0, \dots, 0]$ because the ISI is mainly at the edge of a symbol in the time domain. Note that OCDM can be viewed as a special case of the proposed GCS-based OCM with $\alpha = 1$ multiplying a constant. From Fig. 2, it is seen that the ISI/ICI power distribution varies as α changes. In OCDM, the ISI/ICI power concentrates around the subcarrier #104. In contrast, in GCS-based OCM, there are α peaks in the ISI profile and the interval between peaks is N/α . It is also seen that as α increases, the peak power of the ISI/ICI decreases so that the power is distributed more evenly over subcarriers. Therefore, the ISI can be whitened by using a GCS with a large α , which is expected to improve the performance.

Experimental Setup

The experimental setup is shown in Fig. 1. The numbers of total and modulated subcarriers were 232 and 512, respectively. The frequency of the DUC was set as 118/512 of the sampling rate of the arbitrary waveform generator (AWG), which varied from 54 GSa/s to 65 GSa/s for investigation. The bandwidth of the AWG was 25 GHz while that of the Mach-Zehnder modulator (MZM) was 23 GHz. The fiber length in the experiment was 2 km. At the receiver, a variable optical attenuator (VOA) was used to control the received optical power. The signal was detected by a 10-GHz receiver and sampled by an 80-GSa/s real-time oscilloscope (RTO). The overall system bandwidth was limited by the receiver with the 3-dB bandwidth of ~ 10 GHz and the 15-dB bandwidth of ~ 27 GHz.

For comparison, we also implemented COFDM, DFT-S OFDM, OCDM, and CLPS-based OCM with the optimal $e = [0, 0.25]$ [5]. In all schemes, 16QAM was used and equalization was realized using the zero-forcing method.

Experimental Results

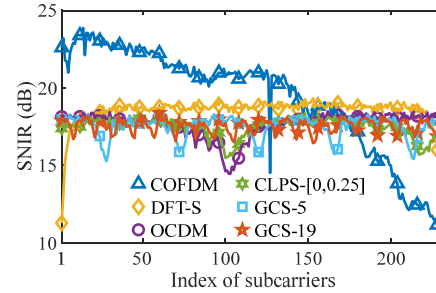


Fig. 3. Estimated SNIR versus the index of subcarriers for different schemes at 112.4 Gbit/s.

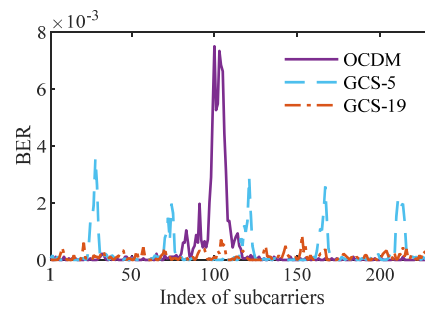


Fig. 4. BER versus the index of subcarriers for the proposed scheme with different α . The data rate is 112.4 Gbit/s.

Fig. 3 shows the estimated SNIR versus the index of subcarriers at 112.4 Gbit/s when the length of CP is 20. It is seen that the SNIR of the COFDM degrades as the subcarrier index increases due to the bandwidth limitation effect. The SNIR of DFT-S OFDM exhibits a deep dip at edge subcarriers due to severe ISI in the experiment. On the other hand, the dips in the SNIR profile of OCDM and CLPS-based OCM are not as severe as that in DFT-S OFDM. By using the proposed

GCS-based OCM, the deep dip splits into α smaller dips, which match the analysis in Fig. 2. When α is 19, the SNIR is much flatter than those in other schemes although slight fluctuation still exists. Fig. 4 shows the BER versus the index of subcarrier for different α . The BER around subcarrier #104 is very high in OCDM. By using GCS-based OCM with $\alpha = 19$, the BER is similar across the subcarriers and the overall BER is significantly reduced.

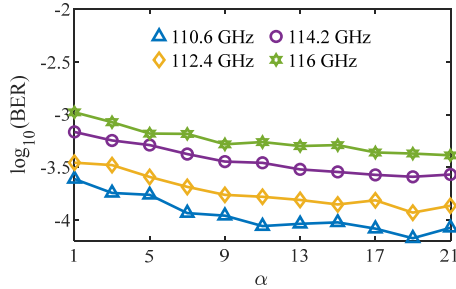


Fig. 5. BER versus the parameter α for the proposed scheme at different data rates.

We further investigate the effect of α by measuring the BER versus α at different data rates, as shown in Fig. 5. It is confirmed that the BER reduces as α increases regardless of the data rate, since the ISI can be whitened in a better way. Note that the performance saturates after a certain α .

Fig. 6 shows the BER performance versus the received optical power (ROP) at 112.4 Gbit/s. When the ROP is small, the system is noise-limited so that the performances of DFT-S OFDM, OCDM, CLPS- and GCS-based OCM are similar, all better than that of COFDM. However, as the ROP increases, the influence of ISI/ICI becomes prominent and the difference of these schemes is visible. The performance of DFT-S OFDM is the poorest because its SNIR profile deviates from the whitened one the most due to the deep dip at edge subcarriers. OCDM and CLPS-based OCM improve the performance but they are still not optimal. The performance of the proposed GCS-based OCM varies with α and is the best when α is selected as a larger value of 19. This matches the analysis in Figs. 3-4 because the ISI/ICI is better whitened and is almost evenly distributed over subcarriers.

Fig. 7 shows the BER versus the length of CP at 112.4 Gbit/s and 2-dBm ROP. In IM/DD, the ISI/ICI cannot be fully eliminated even with a large CP length due to the interplay of severe bandwidth limitation and square-law detection. Therefore, GCS-based OCM using α of 19 still exhibits a performance gain over other schemes under a large length of CP. Fig. 8 depicts the BER versus the bit rate for different schemes when the length of CP is 20 and the ROP is 2 dBm. It is

seen that the performance degrades as the bit rate increases. However, at all data rates, the proposed scheme with α of 19 has better performance than COFDM, DFT-S OFDM, OCDM and CLPS-based OCM, and 117.8-Gbit/s data rates can be achieved for a BER below 10^{-3} .

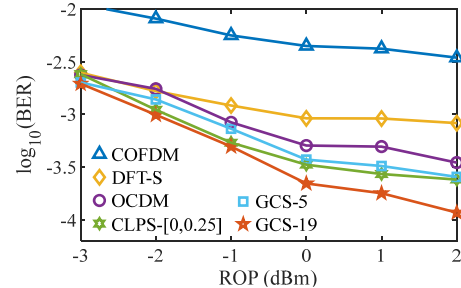


Fig. 6. BER versus the received optical power at 112.4 Gbit/s. The CP length is 20.

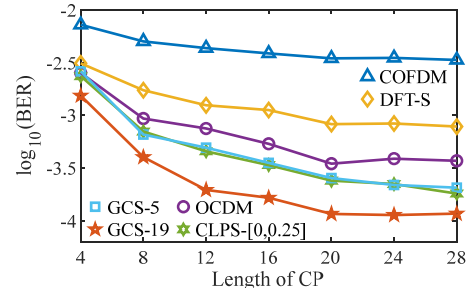


Fig. 7. BER versus the length of CP at 112.4 Gbit/s.

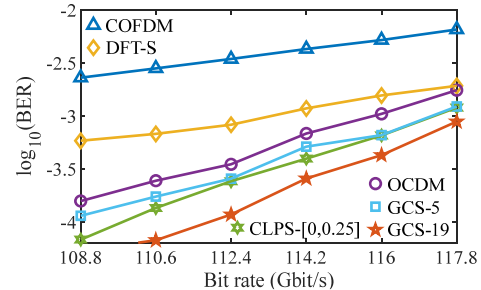


Fig. 8. BER versus the bit rate.

Conclusion

We have proposed a novel GCS-based OCM for bandwidth-limited IM/DD systems. The proposed scheme can control the distribution of ISI over the subcarriers using the parameter α , and so can whiten both the noise and the ISI/ICI enabling a flatter SNIR profile. 108.8~117.8-Gbit/s IM/DD experiments with 10-GHz-class devices show that the proposed scheme achieves better performance than COFDM, DFT-S OFDM, OCDM, and CLPS-based OCM regardless of the ROP, the length of CP and the data rate.

Acknowledgements

National Natural Science Foundation of China (61971199) and Guangdong Basic and Applied Basic Research Foundation (2021A1515012309).

References

- [1] T. Bo, B. Kim, Y. Yu, D. Kim and H. Kim, "Generation of broadband optical SSB signal using dual modulation of DML and EAM," *IEEE Journal of Lightwave Technology*, vol. 39, no. 10, pp. 3064-3071, 2021. DOI: [10.1109/JLT.2021.3058161](https://doi.org/10.1109/JLT.2021.3058161)
- [2] X. Chen, J. Cho, G. Raybon, D. Che, K.W. Kim et al., "Single-Wavelength and Single-Photodiode 700 Gb/s Entropy-Loaded PS-256-QAM and 200-GBaud PS-PAM-16 Transmission over 10-km SMF," *European Conference on Optical Communications (ECOC)*, 2020, paper Th3A.2. DOI: [10.1109/ECOC48923.2020.9333201](https://doi.org/10.1109/ECOC48923.2020.9333201)
- [3] D. Zou, Z. Li, Y. Sun, F. Li, and Z. Li, "Computational complexity comparison of single-carrier DMT and conventional DMT in data center interconnect," *Optics Express*, vol. 27, no. 12, pp. 17007-17016, 2019. DOI: [10.1364/OE.27.017007](https://doi.org/10.1364/OE.27.017007)
- [4] X. Ouyang and J. Zhao, "Orthogonal chirp division multiplexing," *IEEE Transactions on Communications*, vol. 64, no. 9, pp. 3946-3957, 2016. DOI: [10.1109/TCOMM.2016.2594792](https://doi.org/10.1109/TCOMM.2016.2594792)
- [5] Z. Fan and J. Zhao, "Orthogonal Circulant Multiplexing based on the Chirp-Like Polyphase Sequence in Short-Reach IM/DD Systems," *Optical Fiber Communication Conference (OFC)*, 2021, paper Th4D.1. DOI: [10.1364/OFC.2021.Th4D.1](https://doi.org/10.1364/OFC.2021.Th4D.1)
- [6] R. Bomfin, M. Chafii, A. Nimr, and G. Fettweis, "A robust baseband transceiver design for doubly-dispersive channels," *IEEE Transactions on Wireless Communications*, vol. 20, no. 8, pp. 4781-4796, 2021. DOI: [10.1109/TWC.2021.3062263](https://doi.org/10.1109/TWC.2021.3062263)
- [7] F. Berggren and B. Popovic, "Chirp-convolved data transmission," *IEEE Communications Letters*, vol. 25, no. 4, pp. 226-230, 2021. DOI: [10.1109/LCOMM.2020.3042850](https://doi.org/10.1109/LCOMM.2020.3042850)
- [8] X. Ouyang, G. Tall, M. Power, and P.D. Townsend, "Experimental demonstration of 112 Gbit/s orthogonal chirp-division multiplexing based on digital up-conversion for IM/DD systems with improved resilience to system impairments", *European Conference on Optical Communication (ECOC)*, 2018, paper Mo4F.3. DOI: [10.1109/ECOC.2018.8535558](https://doi.org/10.1109/ECOC.2018.8535558)